Probable Unimportance of Intramolecular Hydrogen Bonds for Determining the Secondary Structure of Cyclic Hexapeptides. Roseotoxin B

James P. Snyder

Contribution from Molecular Systems, Merck Sharp & Dohme Research Laboratories, Rahway, New Jersey 07065. *Received April 29, 1983*

Abstract: Roseotoxin B, a cyclic hexadepsipeptide with two unambiguous cross-ring hydrogen bonds expressed as part of a pair of β-turns, has previously been subjected to three separate X-ray determinations. An analysis of the crystal structures in conjunction with molecular mechanics calculations (MM2) demonstrates that the 19-membered backbone ring is readily distorted by low energy torsions about the Cα–Cβ bond of the isoleucine *sec*-butyl side chain. The accompanying cross-ring steric repulsions are the cause of the ring breathing. Molecular surface calculations permit an evaluation of internal N—H···O=C exposure to solvent and yield a consistent interpretation of the combined X-ray and NMR data for the hydrogen bonds. The shorter H bond appears more accessible to solvent as a result of an average torsional shielding of the longer bond by the *sec*-butyl group. These observations imply that the cross-ring bridges do not significantly rigidify the backbone conformations but are instead a consequence of them. This view is supported by additional force-field calculations for structures in which the hydrogen bonds have been eliminated. Conformational integrity is maintained, and the hydrogen bonds are indicated to impart rather minor local geometrical effects on the overall structure.

Cyclic peptides are frequently encountered natural products exhibiting a wide variety of essential biological functions.[1] Synthetic derivatives are sought for their utility as drug candidates,[2] for case studies of conformational analysis,[3] and as models for large peptides and proteins.[4] The growing list of X-ray and NMR investigations[5,6] focused on peptide rings containing 9–36 members almost universally depicts structures with 3→1 or 4→1 cross-ring hydrogen bonds. Equally ubiquitous is the assumption, often explicit, that the hydrogen bonds are crucial as structural determinants of the cyclic peptides. The lore of β and γ turns[6,7] is applied generously to these structures and has been accompanied by a considerable effort to distinguish intra- and intermolecular hydrogen bonding by NMR.[6,8]

It appeared desirable to explore the structural role of hydrogen bonding in a cyclic peptide of moderate size for which X-ray data are available. Furthermore, certain interpretive amgibuities are avoided if *intra*molecular H bonds are well expressed, but *inter*molecular interactions in the crystal are absent. Roseotoxin B, a toxic metabolite arising from the action of the fungus *Trichothecium roseum* found on moldy peanuts,[9] suits the present purpose admirably. The compound **1**/**1′** is a 19-membered ring for which three separate X-ray structures have been determined.[9] Intermolecular hydrogen bonding is not a feature of the crystals; packing appears to be a result of van der Walls and long-range electrostatic forces alone.

In the work described below, the crystal structures are analyzed in detail along with supplementary force-field calculations. Side-chain rotation is observed to promote low-energy ring backbone breathing. Ultimately the conclusion is drawn that the basic ring conformation is only weakly influenced by the presence of cross-ring H bonds.

Methods and Results

X-ray Structures. The X-ray determinations for **1**/**1′** (Figure 1) arise from three crystal modifications of $P2_1$ cell symmetry.

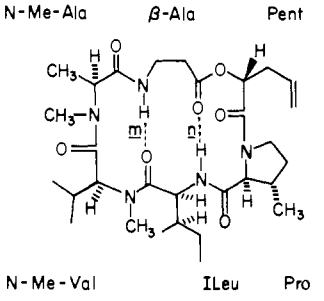

1

Crystals grown from ether–hexane were evaluated at 138 K (REH-LT) and room temperature (REH-RT). Benzene-derived crystals were likewise studied at ambient temperature (RB-RT). The first was refined with hydrogens; the latter two, without. Corresponding unweighted *R* factors are 0.039, 0.092, and 0.089, respectively.[9]

Each of these structures was examined in detail on an Evans and Sutherland multipicture system configured to a VAX 11/780 and supported by the Merck molecular modeling software.[10] For REH-LT the average positions of the atoms in the *N*-Me-Val and Ile hydrocarbon side chains led to a number of unrealistic H–C–H

(1) (a) Ovchinnikov, Y. A.; Ivanov, V. T. *Tetrahedron* **1975**, *31*, 2177–2210. Hruby, V. J. "Topics in Molecular Pharmacology"; Burgen, A. S. V.; Roberts, G. C. K., Eds.; Elsevier/North-Holland: New York, 1981; pp 99–126. (b) Kessler, H. *Angew. Chem. Int. Ed. Engl.* **1982**, *21*, 512–523.

(2) Veber, D. F.; Holly, F. W.; Nutt, R. F.; Bergstrand, S. J.; Brady, S. F.; Hirschmann, R.; Glitzer, M. S.; Saperstein, S. *Nature (London)* **1979**, *280*, 512–514. Veber, D. F.; Freidinger, R.; et al. *Ibid.* **1981**, *292*, 55–58.

(3) Bovey, F. A.; Brewster, A. I.; Patel, D. J.; Tonelli, A. E.; Torchi, D. A. *Acc. Chem. Res.* **1972**, *5*, 193–200. Scheraga, H. "Peptides: Proceedings of the Fifth American Peptide Symposium"; Goodman, M., Meienhofer, G., Eds.; Wiley: New York, 1977; pp 246–256. Scheraga, H. A. "Peptides, Polypeptides and Proteins"; Blout, E. R., Bovey, F. A., Eds.; Wiley-Interscience: New York, 1974; pp 49–70. Kessler, H. "Stereodynamics of Molecular Systems"; Sarma, R. H., Ed.; Pergamon Press: New York, 1979; pp 187–196.

(4) Deber, C. M.; Madison, V.; Blout, E. R. *Acc. Chem. Res.* **1976**, *9*, 106–113. Blout, E. R. *Biopolymers* **1981**, *20*, 1901–1912. Gierasch, L. M.; Deber, C. M.; Madison, V.; Niu, C. H.; Blout, E. R. *Biochemistry* **1981**, *20*, 4730–4738.

(5) a) Karle, I. L. "The Peptides, Analysis, Synthesis, Biology"; Gross, E., Meienhafer, J., Eds.; Academic Press: New York, 1981; Vol. IV, pp 1–53. b) Benedetti, E. "Peptides, Proceedings of the Fifth American Peptide Symposium"; Goodman, M., Meienhofer, J., Eds.; Wiley: New York, 1977; pp 257–272.

(6) Smith, J. A.; Pease, L. G. *CRC Crit. Rev. Biochem.* **1980**, *8* (4), 315–399.

(7) Venkatachalam, C. M. *Biopolymers* **1968**, *6*, 1425–1426. Chandrasekaran, R.; A. V. Lakshminarayan, Pandya, U. V.; Ramachandran, G. N. *Biochim. Biophys. Acta* **1973**, *303*, 14–27.

(8) Kopple, K. D.; Schamper, T. J. "Chemistry and Biology of Peptides"; Meienhofer, J., Ed.; Ann Arbor Science: Ann Arbor, MI, **1972**; p 75.

(9) Springer, J. P.; Cole, R. J.; Dorner, J. W.; Cox, R. H.; Richard, J. L.; Barnes, C. L.; v.d. Helm, D. *J. Am. Chem. Soc.*, preceding paper in this issue.

(10) Gund, P.; Andose, J. D.; Rhodes, R. B.; Smith, G. M. *Science Washington D.C.* **1980**, *208*, 1425–1431.

0002-7863/84/1506-2393$01.50/0

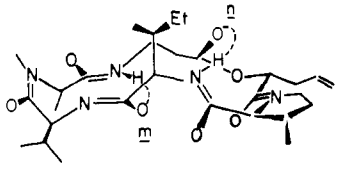

Figure 1. Three-dimensional view of roseotoxin B (**1′**) illustrating its crownlike shape and showing the bend directions for intramolecular hydrogen bonds *m* and *n*. The amide groups are drawn in their enol representations to emphasize the importance of the stiff planar units for the overall molecular conformation.

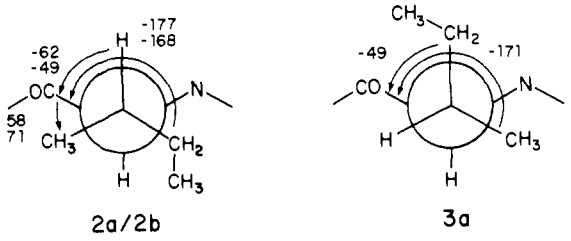

Figure 2. X-ray determined conformations for rotation about the Cα–Cβ bond at the *sec*-butyl Ile side chain in roseotoxin B; deg. On the left, values are listed in descending order **a**:**b**.

bond angles. It is not uncommon to find larger uncertainties in atomic positions at the extremities of molecules of moderate to large size.[11] These were regularized with the Molecular Editor to near tetrahedral values. The resulting structure will be referred to as **2a**. REH-RT was reported with 120–125° bond angles around the β-CH_3 of the Ile side chain. The angles were modified to intuitively reasonable values (CH_3–CH–CN, 108°; CH_3–CH–CH_2, 112°) and hydrogens were added to the entire structure with the HGROW procedure[10] to give **2b**. The third set of X-ray coordinates, RB-RT, were used unchanged though supplemented with hydrogens by HGROW yielding **3a**.

It will be noted that structures **2a** and **3a** differ importantly in that they correspond to different conformations about the *sec*-butyl Cα–Cβ bond at Ile. Figure 2 illustrates that **2a**/**2b** experience two gauche-type interactions, while **3a** shows three of them. Comparison of **2a** and **3a** likewise reveals a different spatial orientation of the propenyl side chain at the 2-hydroxypentenoyl residue. Both of these conformational features were highlighted by the authors of the X-ray work.[9]

Force-Field Calculations: MM2. In order to evaluate the impact of *sec*-butyl conformation on the structure of roseotoxin B, both **2a** and **3a** were fully geometry optimized with the Allinger MM2 method[12a,b] employing parameters derived largely by the Marshall group.[12c] The resulting structures are labeled **2c** and **3b**, respectively. In addition, the *sec*-butyl side chain of **2a** was manipulated by a rigid rotation to the same dihedral angle as that of **3a** (Figure 2). This construct was then optimized to give structure **3c**. In this way the conformations are placed on the same geometry-energy scale and thereby suitable for comparison with one another and related but unknown structures. Several other calculations were also performed. Thus, the *N*-CH_3's at *N*-Me-Ala and *N*-Me-Val in **2a** were compressed to NH's and the resulting peptide was optimized to produce **4c**. Depsipeptide **5** resulted from replacement of the β-Ala NH in **1**/**2a** with oxygen accompanied by MM2 refinement. Similarly, the bis-lactone **6** arose by substitution of both β-Ala and Ile NH's by oxygen followed by energy relaxation. Related modifications apply to structures **7** and **8**.

Table I. Dihedral Angles for X-ray and MM2 Determined Conformations of Roseotoxin B[a]

		2a[b]	2b[c]	2c[d]	3a[e]	3b[f,h]	3c[g,h]
Ile,	φ	−79	−92	−76	−120	−77	−76
	ψ	144	150	135	158	148	144
	ω	171	175	168	169	−179	−172
Val,	φ	−100	−98	−92	−91	−98	−100
	ψ	101	109	95	116	98	99
	ω	6	1	22	16	22	19
Ala,	φ	−128	−127	−138	−136	−142	−138
	ψ	112	104	84	67	84	83
	ω	177	179	178	−173	172	175
β-Ala,	θ1	−138	−128	−115	−106	−107	−103
	θ2	−77	−79	−72	−87	−70	−66
	θ3	168	169	171	−178	−174	164
	LACTONE	174	173	174	170	172	174
Pent,	φ	65	67	53	68	49	53
	ψ	−135	−137	−127	−136	−128	−128
	ω	−178	−177	−175	−172	−171	−167
Pro,	φ	−80	−85	−81	−90	−82	−77
	ψ	−10	−2	−17	11	−33	−35
	ω	180	179	179	180	−177	179
Ile side chain							
CO–Cα–Cβ–CH_3		58	71	67	−171	169	170
CO–Cα–Cβ–CH_2		−177	−168	−166	−49	−66	−65
CH_3–Cβ–CH_2–CH_3		75	59	71	−73	−64	−65
Cα–Cβ–CH_2–CH_3		−51	−59	−57	166	171	171

[a] In degrees. Twice the estimated standard deviations for the dihedral angles are 2a, 0.4–0.8°, 2b/3a, 1.2–1.8°; cf. ref 9. [b] REH-LT/X-ray with some regularized H–C–H angles in the Ile and Val side chains. [c] REH-RT/X-ray with regularized β-CH_3 angles in the Ile side chain. [d] 2a after MM2 optimization. [e] RB-RT/X-ray. [f] 3a after MM2 optimization. [g] 2a with 3a Ile side-chain conformation after MM2 optimization. [h] Cf. ref 22.

Finally, **2b** (REH-RT) was processed by MM2, but it settled in the same conformation as that derived from **2a** (REH-LT), i.e., **2c**.

Backbone and Ile *sec*-butyl dihedral angles for **2**–**8** are reported in Tables I and V. Hydrogen bond geometries are presented in Table II. Figures 3 and 4 exhibit H···H, H···O, C···C, and N···C cross-ring distances for both the X-ray and the force-field structures. Analysis of the data indicates that while certain backbone dihedral angles common to the experimental and calculated structures are not satisfactorily matched, the overall conformations are in fact quite similar. Figure 5 represents the situation with computer drawn images at selected viewing angles. Equally compelling are the cross-ring distance comparisons of Figures 3 and 4. The MM2 structures **2c** and **3b** mimic the X-ray results both qualitatively and semiquantitatively. The distance differences in the latter figure are particularly satisfying and provide confidence in the MM2 methodology's ability to describe accurately the structural details of molecules in the roseotoxin class.

Molecular Surface Area Calculations. For the purpose of analyzing the degree to which the NH protons in hydrogen bonds *m* and *n* in **1**/**1′** are "exposed" to solvent, molecular surface areas (Å^2) for structures **2**–**4** were carried out. Connolly's algorithm[13] using MM2 van der Waals radii[12a,b] was employed. Qualitative aspects of the calculations are shown in Figure 6. The evaluation of a surface is accomplished by rolling a molecular probe across the structure in question represented as the envelope of a set of interpenetrating spheres assigned individual van der Waals radii. Both the "contact" and "reentrant" areas as conceptualized by Richards[14] are calculated and summed to give the "molecular" surface area.[15] Atoms which are near the molecular surface may

(11) (a) Disorder or thermal motion in the crystal is especially effective in increasing the uncertainty of atomic positions near the terminus of peripheral groups. The uncertainties are expressed as averaged positions sometimes leading to unrealistic internal variable values for the static X-ray structure.[11b] In the present case the worst of these have been returned to one of the putative contributors to the average and subsequently used in the comparison. (b) Stout, G. H.; Jensen, L. H. "X-ray Structure Determination"; Macmillan: London, 1968; p 413.

(12) (a) Allinger, N. L. *J. Am. Chem. Soc.* **1977**, *99*, 8127–8134. (b) Allinger, N. L.; Yuh, Y. *QCPE*, **1980**, *12*, 395. (c) Van Opdenbosch, N.; Humblet, C.; Marshall, G. R.; Snyder, J. P. unpublished.

(13) Connolly, M. L. *Science Washington D.C.* **1983**, *221*, 709–713. Merck adaptations by Dr. G. Smith.

(14) Richards, F. M. *Annu. Rev. Biophys. Bioeng.* **1978**, *6*, 151–176.

(15) The "molecular surface" is the boundary of the volume accessible to the surface of the probe sphere, while the term "solvent accessible surface" is the boundary of the volume accessible to the center of the probe sphere. The latter is thus traced out by the radius of a sphere (*R*) which is the sum of the van der Waal's radius of the atom (r_{VDW}) and the radius chosen for the water molecule (r_W; $R = r_{VDW} + r_W$).

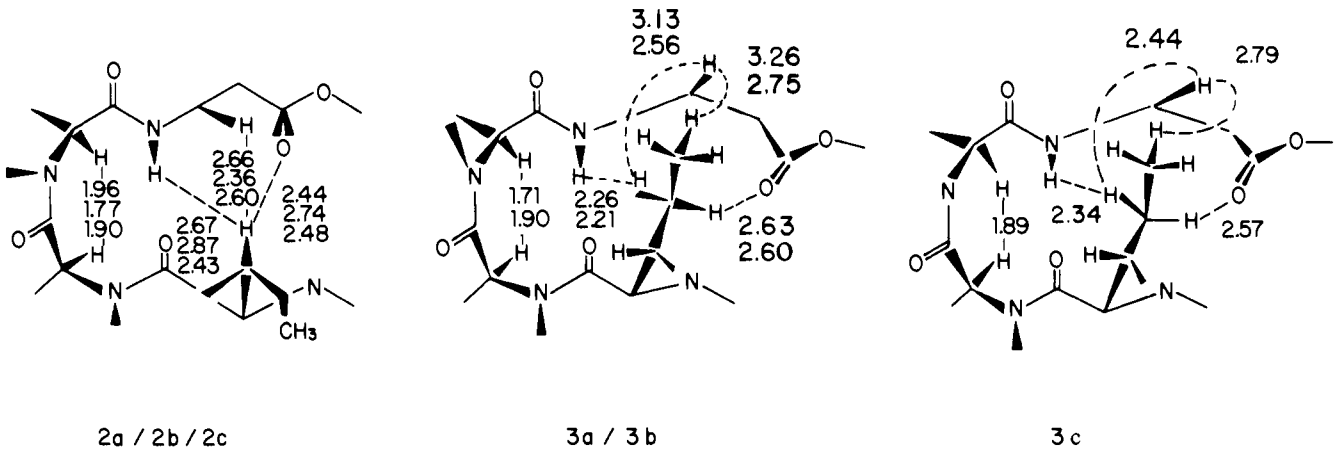

2a / 2b / 2c 3a / 3b 3c

Figure 3. Part structure of roseotoxin B conformations about the Ile *sec*-butyl side chain. **2a**, **2b**, and **3a** are from the X-ray structures REH-LT, REH-RT, and RB-RT, respectively. **2c**, **3b**, and **3c** were derived from MM2 calculations. The distances (Å) correspond to the shortest cross-ring H···H and H···O contacts for **2** and **3**. The values are listed in descending order **a**:**b**:**c**.

Table II. Hydrogen Bond Geometries for X-ray- and MM2-Derived Conformations of Roseotoxin B (**2**/**3**) and the MM2-Derived Depsipeptides 4c, 5, and 6 (Å, deg[a])

	2a	2b	2c	3a	3b	3c	4c	5	6
(β-Ala)NH/(Ile)CO									
*r*N···O (*m*)[b]	2.824	2.859	2.716	2.974	2.957	2.842	2.683	2.902[c]	2.961[c]
*r*N–H···O	1.902	(1.929)	1.769	(1.985)	2.019	1.895	1.756		
∠N–H···O	173	(154)	168	(170)	165	168	161		
(Ile)NH/(β-Ala)CO									
*r*N···O (*n*)[b]	3.033	3.123	2.934	3.230	3.240	3.402	2.983	3.064	3.290[d]
*r*N–H···O	2.181	(2.197)	2.121	(2.243)	2.597	2.707	2.134	2.241	
∠N–H···O	161	(153)	142	(169)	125	130	147	143	

[a] Parenthetical values refer to NH hydrogen positions arising by placement of hydrogens on the X-ray structures with standard bond lengths and angles (i.e., HGROW; ref 10). [b] Twice the estimated standard deviations are **2a**, 0.004–0.008; **2b**, 0.012–0.044; **3a**, 0.012–0.042 Å; cf. ref 9. [c] *r*((β-Ala)O···O=C(Ile)). [d] *r*((Ile)O···O=C(β-Ala)).

Table III. Molecular Surfaces of Roseotoxin B Structures Derived from X-ray Crystallography and Force-Field Optimization (MM2) Using a Surface Probe of Radius 1.4 and 0.0 Å[a,b]

H-bond *m*	probe radius, *r* = 1.4 Å								probe radius, *r* = 0.0 Å							
	O = C – N – H ··· O = C – N – H								O = C – N – H ··· O = C – N – H							
2a	17.2	3.6	3.6	1.2	9.1	0.0	0.0	5.6	27.0	8.6	7.1	4.7	18.6	2.9	0.8	9.2
2b	17.1	1.9	0.0	1.9	5.6	0.0	0.0	3.3	16.0	4.0	4.7	3.5	10.6	4.0	0.8	2.9
2c	18.3	0.0	0.0	0.0	6.2	0.0	0.0	3.6	28.1	4.7	5.1	2.1	15.7	2.9	2.0	4.3
3a	20.0	1.6	0.0	0.0	9.1	5.0	0.0	3.7	30.2	5.6	3.5	2.1	17.9	9.3	2.0	7.3
3b	15.9	0.0	2.7	0.0	2.7	0.0	0.0	3.3	26.1	4.7	7.0	1.1	10.3	3.6	2.4	6.2
4c	18.9	2.7	1.6	2.0	2.7	0.0	0.0	6.7	18.6	6.1	4.3	2.5	9.1	4.0	1.6	8.5
H-bond *n*	O = C – N – H ··· O = C – O								O = C – N – H ··· O = C – O							
2a	21.4	0.7	0.0	0.0	4.7	0.8	8.1		34.7	5.8	0.4	1.1	11.9	6.2	17.2	
2b	21.5	2.4	0.0	0.0	5.1	1.9	12.0		17.9	5.8	1.2	0.7	8.0	5.0	8.7	
2c	18.7	0.0	0.0	0.0	2.4	1.9	13.4		31.6	4.3	0.8	0.0	7.7	7.3	22.9	
3a	16.7	2.7	0.0	0.0	3.6	3.2	4.4		25.8	6.0	2.0	1.8	11.2	8.2	12.4	
3b	19.5	0.0	0.0	0.0	1.6	5.2	14.6		34.3	4.0	2.4	0.4	6.2	10.2	15.7	
4c	20.4	0.0	0.0	0.0	5.2	0.8	13.1		19.4	4.3	0.8	0.7	6.5	5.0	11.0	

[a] Values listed correspond to atoms in amides involved in hydrogen bonds *m* and *n*; in Å². [b] Van der Waals radius for H in N–H is 1.5 Å.

not register a contribution to it if the probe radius is too large to permit a full exploration of the surface crevices. In the present work a probe radius of 1.4 Å was utilized to mimic the size of a spherical water molecule in contact with the various roseotoxin B conformations. Other values for the probe radius have been made in various applications,[16-18] but the results are not partic-

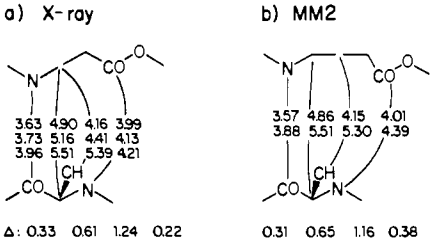

Figure 4. Part structure of roseotoxin B conformations showing selected cross-ring backbone atom distances in Å. (a) X-ray: the distances for conformations **2a** (REH-LT, upper number), **2b** (REH-RT), and **3a** (RB-RT, lower). The values below the structure are the differences in cross-ring distance for **2a** and **3a** (Å). (b) MM2: same comparison for the force-field optimized structures **2c** and **3b**.

(16) Lee, B.; and Richards, F. M.; *J. Mol. Biol.* **1971**, *55*, 379–400.
(17) Ponnuswamy, P. K.; Manavalan, P. *J. Theor. Biol.* **1976**, *60*, 481–486. Manavalan, P.; Ponnuswamy, P. K.; Srinivasan, A. R. *Biochem. J.* **1977**, *167*, 171–182. Genest, M.; Vovelle, F.; Ptak, M. *J. Theor. Biol.* **1980**, *87*, 71–84. Vovelle, F.; Genest, M.; Ptak, M.; Maigret, B.; Premilat, S. *Ibid.* **1980**, *87*, 85–95.
(18) Hermann, R. B. *J. Phys. Chem.* **1972**, *76*, 2754–2759. Chothia, C. *Nature* (*London*) **1975**, *254*, 304–308. Greer, J. Bush, B. L. *Proc. Natl. Acad. Sci. U.S.A.* **1978**, *75*, 303–307. Janin, J. Chothia, C. *Biochemistry* **1978**, *17*, 2943–2948. Finney, J. L. *J. Mol. Biol.* **1978**, *119*, 415–441.

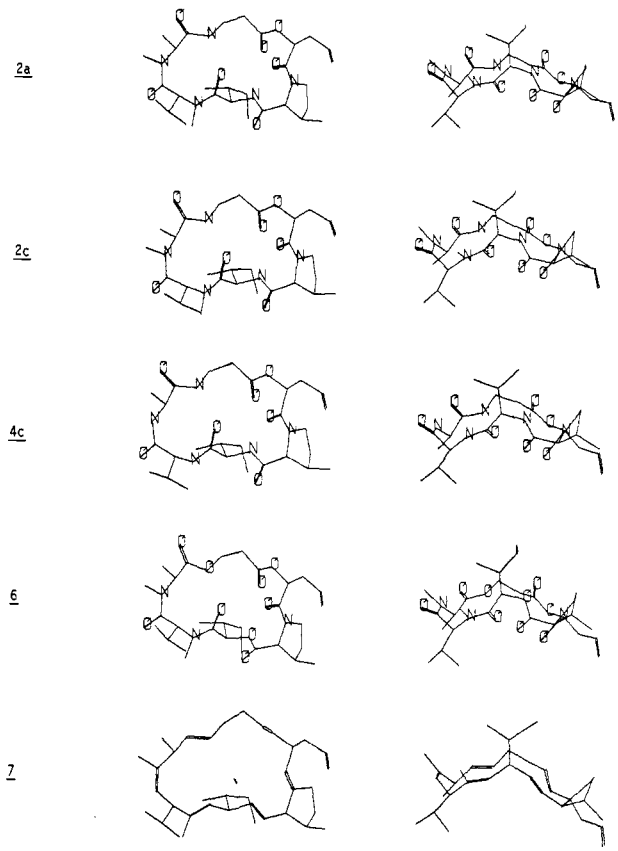

Figure 5. Two computer-drawn views of roseotoxin B (REH-LT, **2a**), the MM2-optimized conformation **2c**, the demethylated structure **4c**, triple dipsipeptide **6**, and hydrocarbon **7**.

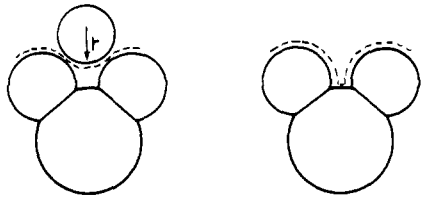

Figure 6. Molecular surface areas calculated by rolling a probe across an assembly of atoms represented by any set of van der Waals radii. The surface arising from a probe with finite radius, r, is shown to the left; that with a probe of 0 radius, to the right.

ularly sensitive to the choice. Table III lists the surface contributions (Å^2) of the atoms involved in the two cross-ring hydrogen bonds m and n. It is seen that a number of atoms are untouched by the water probe. To allow a more detailed comparison of the two hydrogen bonds, a second set of calculations with a probe radius of 0 was performed (Table III, Figure 6). It needs to be emphasized that the molecular surface areas utilized in the present analysis correspond to the van der Waals surfaces as depicted in Figure 6 and not to the "accessible surface areas" as defined by Lee and Richards.[15,16] Were the latter surfaces employed in the present evaluation, no distinction between hydrogen bonds m and n (**1**/**1**′) in **3a** could be made, as is evident from the tabulation for a probe radius of 1.4 Å in Table III. Likewise, an equally uninformative comparison of the two cross-ring hydrogen bonds would arise for **2a** and **2b** since the N–H in bond n shows no contribution to the calculated molecular surface (Table III).

Discussion

Structure of Roseotoxin B. Roseotoxin (B) (**1**) is a 19-membered ring composed of a hydroxy acid and five amino acids. The alanine and valine residues are N-methylated. Seven chiral centers are found in the molecule, five in the main 19-membered ring and one each in the proline and isoleucine side chains. The overall shape of the ring resembles that of a crown (Figure 1) somewhat similar to that ordinarily pictured for cyclooctane. The ester and amide links are trans with the exception of the cis configuration between *N*-methylvaline and *N*-methylalanine shown to the left in **1**/**1**′. Two well-developed hydrogen bonds, m and n, with good geometric characteristics span the structure and divide it into three rings of 10, 11, and 10 members. The 10-membered proline-containing ring on the right of **1**/**1**′ constitutes a classic 4→1 trans or type II′ β-turn. The 10-ring on the left is a 4→1 cis connection. As is illustrated in **1**′, the hydrogen bonds bow away from the average plane of the molecule in different directions.

A remarkable and fortunate feature of the X-ray determinations is the finding that the Ile *sec*-butyl side chain has been captured in two conformations in the solid state (Figure 2) as a result of changing the crystallization solvents from benzene to ether–hexane.[19] In **2a**/**2b** (REH-LT/RT) the ethyl group is directed outside the peptide ring, whereas in **3a** it resides over the central 11-membered ring. The immediate implication is that the energy of the two conformations must be very similar. Indeed, comparison of the MM2 optimized versions places **3b** 2.5 kcal above **2c**. Rotation of the *sec*-butyl side chain in **2a** to that in **3a** (Figure 2) followed by geometry relaxation leads to **3c**, only 0.3 kcal above **2c** (cf. Figure 3).

Influence of the Ile *sec*-Butyl Conformation on Ring Backbone Shape. The distances given in Figure 3 make it clear that conformation **2** experiences steric compression between the hydrogen at the tertiary center of *sec*-butyl and several atoms in the β-alanine residue. The sum of the H···H and H···O van der Waals radii either according to Bondi[21] (2.40/2.72 Å, respectively) or to the more stringent Allinger[12a] prescription (3.00/3.24 Å, respectively) is to be compared with the 2.66, 2.67/2.44 Å distances for **2a** (REH-LT) in Figure 3. Rotation of the *sec*-butyl group to place the ethyl moiety over the ring engenders an equally congested environment. Both the CH_2 and CH_3 protons exhibit close contacts with the β-alanine fragment. The pertinent distances for **3a** (RB-RT) are 2.26, 3.13 (H···H), and 2.63 Å (H···O) (cf. Figure 3).

The impact of cross-ring nonbonded contacts on the depsipeptide backbone is illustrated by the atom–atom distances in Figure 4. Ring atoms move from 0.2 to 0.6 Å apart as the *sec*-butyl group is swung over the central ring. The Ile Cβ responds by retreating 1.2 Å. Simultaneously, the cross-ring hydrogen bonds are stretched approximately 0.1–0.2 Å. Dihedral angles for **2a** and **3a** are adjusted accordingly (Tables I and II). Alternatively, the coupled motions can be rationalized as side-chain displacement induced by ring shape changes. Atomic movements are clearly mutual and cooperative.

Force-field optimization faithfully reproduces all of the trends described above as deduced from Figures 3 and 4. Impressively, the cross-ring backbone atom shifts as a function of *sec*-butyl conformation are reproduced quantitatively by the calculations (Figure 4). The remarkable correlation of structural variation within the sets of force-field and X-ray structures would appear to substantiate the corrections made for the latter. One interesting outcome of the MM2 evaluation of **2a** (REH-LT) adapted to mimic the Ile side chain conformation of **3a** (RB-LT) is structure **3c** in Figure 3, a MM2 minimum not observed among the trio of X-ray structures. As mentioned above, **3c** lies only 0.3 kcal over **2c**. Small, coupled adjustments in the MM2-derived dihedral angles throughout the roseotoxin B structure contrive to establish a closely related but different set of close cross-ring interactions. The potential energy surface describing the molecule's flexibility is obviously quite shallow.[22]

(19) Occasionally, two conformations are observed in the same unit cell.[20a–c] More often, closely related conformers with differing substitution patterns are seen from crystal to crystal.[20d]

(20) (a) Karle, I. L.; Karle, J. *Acta Crystallogr.* **1963**, *16*, 969–975. (b) Varughese, K. L.; Kartha, G.; Kopple, K. D. *J. Am. Chem. Soc.* **1981**, *103*, 3310–3313. (c) Winkler, F. K.; Dunitz, J. D. *Acta Crystallogr., Sect B* **1975**, *31*, 281–283. Johnson, C. A.; Guenzi, A.; Nachbar, R. B., Jr.; Blount, J. F.; Wennerström, O.; Mislow, K. *J. Am. Chem. Soc.* **1982**, *104*, 5163–5168. (d) Dunitz, J. D. "X-Ray Analysis and the Structure of Organic Molecules"; Cornell University Press: Ithaca, NY, 1979.

(21) Bondi, A. J. *J. Phys. Chem.* **1964**, *68*, 441–451.

The X-ray analysis of **2b** (REH-LT) brings this point home in another way. Figures 3 and 4 and Table II indicate that cross-ring atom–atom and hydrogen bond distances fall between those for **2a** (REH-LT) and **3a** (RB-RT). The same is the case for the experimental dihedral angles (Table I), as pointed out by the authors of the structural work.[9] The origin of the intermediate values is not as clear-cut as the progression from **2a** to **3a**. A much more subtle effect may be in operation. Figure 2 displays the differences between **2a** and **2b**. The latter relative to the former shows a 12° rotation of the *sec*-butyl group in the direction of **3a**. Given the tight distances between cross-ring atoms and the apparent flatness of the molecular energy surfaces in response to *sec*-butyl rotation, a full-molecule geometric adjustment to the slight twist is conceivable and consistent. Unfortunately, the experimental distances measured for hydrogen are less predictive in this interpretive context for reasons given in the Results section.

Alternatively the **2a**/**2b** differences can be interpreted as a consequence of either static disorder or thermal motion in the room-temperature crystals. Although indistinguishable, in either case the **2b** *sec*-butyl fragment geometry is then an average of a range of positions from molecule to molecule. An analysis of the temperature factors for **2a**, **2b**, and **3a** is supportive.[11a] Only **2b** possesses extraordinarily large thermal parameters for the atomic coordinates associated with the Ile side chain.[9] The computational observation that structure **2b** (REH-RT) relaxes to the geometry of **2a** (REH-LT) when subjected to an unconstrained MM2 optimization is fully consistent. Again, though there are distinct energy minima on the conformational energy surface, they would appear broad and susceptible to being easily traversed.

Two conclusions are permissible from the foregoing discussion. Firstly, neither crystal packing nor dominant temperature effects[9] need be invoked to rationalize the ring or side-chain conformational mobility found for the crystal structures **2a**, **2b**, and **3a**, all of which are free of intermolecular hydrogen bonding. Cross-ring steric effects alone can assume responsibility for the ring dislocations. These arise naturally out of both the geometric analysis and the conformational energy calculations. Secondly, the hydrogen bonds in **1**/**1′** (*m* and *n*) seem indifferent to distortion. Conversely, if this indeed be the case, the conformational flexibility of the 19-membered ring dipsipeptide is equally indifferent to the presence of hydrogen bonds *m* and *n*. This notion will be explored from two other viewpoints below.

Solvent Exposure of the N–H Hydrogen Bonds. In methanol solvent the β-alanine NH is shifted downfield in the NMR by 0.3 ppm relative to its position in chloroform. The Ile NH is unchanged by the switch in solvent.[9] This observation is in harmony with related NMR characteristics observed for destruxin B (**4a**) and its desmethyl congener **4b**. These substances differ slightly from roseotoxin B in that the allyl side chain at carbon α to the lactone (**1**) is replaced by a *sec*-butyl moiety. Secondly, the methyl group at proline is absent. For the desmethyl derivative, the valine residue possesses an NH.

In addition to the $CDCl_3 \rightarrow$ MEOD NH chemical shift, the β-alanine and Ile NH's in Me_2SO show a weak temperature dependence[23] characteristic of internal NH protons[6] (i.e.,

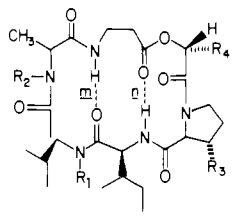

	R_1	R_2	R_3	R_4
1	CH_3	CH_3	CH_3	CH_2-CH=CH_2
4a	CH_3	CH_3	H	$CH_2CH(CH_3)_2$
4b	H	CH_3	H	"
4c	H	H	CH_3	CH_2-CH=CH_2
4d	H	H	H	CH_2-$CH(CH_3)_2$

$-(\Delta\delta/\Delta T) \times 10^{-3}$: **4a**/**4b** Ile 0.3/0.5, β-Ala 1.0/1.7, Val 5.3). Furthermore, the NH protons undergo H–D exchange in the following order: Val > β-Ala > Ile.[23] If conformational constancy from $CDCl_3$ to Me_2SO is assumed, the NMR measurements are in complete accord with the X-ray data in that they place the Ile and β-Ala protons inside the roseotoxin/destruxin ring structure and the Val NH hydrogen external to it.

In the present discussion, the relative disposition of the hydrogen bonds *m* and *n* in **1** is the interesting feature. By the geometric X-ray criterion, the short H bond *m* (β-Ala NH) might be considered stronger. On the basis of the NMR studies, the *n* bond (Ile NH) would appear tighter. Unfortunately, the NMR probes are indirect. They are designed to reflect the existence of *inter*molecular NH hydrogen bonds[6] as in the case of Val in **4b**. The absence of the corresponding indicator is often assumed to mean that an NH is strongly *intra*molecularly H-bonded, though it may simply be shielded from the solvent on structural grounds.[24]

The molecular surface calculations assist in permitting a coherent interpretation for structures **1** and **4**. In the present context, the calculated molecular surface envelopes for the various conformations as symbolized by Figure 6 have been chosen as a crude measure of the variance to solvent exposure for the cross-ring hydrogen bonds *m* and *n* (**1**/**1′**). Similar calculations concerned with predicting the hydration sites for dipeptides have been performed.[17] An additional assumption made here is that solvent exposure is related both to the strength of the molecular association between the solute atoms and the nearby solvent molecules as well as to the relative rates of proton exchange. While this seems intuitively reasonable, it is not yet demonstrable. In fact, if the atomic surfaces of Table III are taken at face value, the N–H of hydrogen bond *n* is seen to be totally unexposed to solvent. The same would be true if Lee and Richards' "static accessibility" criterion[15,16] were applied to roseotoxin B. The supposition that a relationship exists between calculated molecular surfaces and dynamic properties for buried NH protons relies on the knowledge that molecules are not static. Thermal motion within the peptide backbone provides the opportunity for time-dependent access of sequestered protons *m* and *n* to solvent. Conformational interconversion is a second mechanism for bringing internal NH's into contact with the surrounding medium. The relation between the two is appreciated by noting that ring breathing motions occurring near the bottom of potential energy wells are the molecular vibrations which ultimately lead to passage across conformational transition states upon absorption of sufficient thermal energy. Cyclic peptides exhibit energy barriers ranging from 10 to 23 kcal/mol for diverse isomerization processes such as ring inversion,[25] cis–trans amide rotation,[26] and disulfide chirality reversal.[27] By contrast, skeletal vibrations as mirrored by infrared spectroscopy are ordinarily activated at less than 2 kcal/mol.[28] Molecular vibrations with their specific potential for bringing

(22) (a) MM2, employing a modified block-diagonal Newton–Raphson optimizer, seeks energy minima by moving a single atom at a time. The standard version of the program employed throughout the present work yields relative energies for **3b**, **3c**, and **2c** of 2.5, 0.3, and 0.0 kcal. The flatness of the energy surface and the similarity in torsional geometry for **3b** and **3c** (Table I) suggested possible incomplete optimization. Accordingly, the MM2 structures were reoptimized with the same force field coupled to a variable metric optimization procedure[22b] which minimizes the energy by simultaneous atomic movements. The energy gap between **3b** and **3c** fell to 1.1 kcal and the geometric differences were reduced. It may well be that the two structures thus represent the same stationary point (minimum) on a near flat energy plane. It has been pointed out that MM2 in certain cases ought to be supplemented with a more robust optimizer.[22c,d] (b) Halgren, T. A. (CCNY) has implemented MM2 in OPTIMOL, a package designed to evaluate enzyme–inhibitor interactions; private communication. (c) Allinger, N. L.; Flanagan, H. L. *J. Comput. Chem.* **1983**, *4*, 399–403. (d) Nachbar, R. (Merck) has incorporated the MM2 force field into BIGSTRN-3 permitting a full Newton-Raphson treatment of molecular structures (cf. Bürgi, H.-B.; Hounshell, W. D.; Nachbar, R. B., Jr.; Mislow, K. *J. Am. Chem. Soc.* **1983**, *105*, 1427–1438).

(23) Naganawa, H.; Takita, T.; Suzuki, A.; Tamura, S.; Lee, S.; Izumiya, N. *Agric. Biol. Chem.* **1976**, *40*, 2223–2229.

(24) Llinas, M.; Klein, M. P. *J. Am. Chem. Soc.* **1975**, *97*, 4731–4737.

(25) Kessler, H.; Kondor, P.; Krack, G.; Krämer, P. *J. Am. Chem. Soc.* **1978**, *100*, 2548–2550. Rich, D. H.; Bhatnagar, P. K.; *Ibid.* 2218–2224. Deber, C. M.; E. T. Fossell, E. T.; Blout, E. R. *Ibid.* **1974**, *96*, 4015–4017. T. Schaug, *Acta Chem. Scand. Ser. B* **1971**, *25*, 2771–2772.

(26) Dale, J.; Titlestad, K. *Acta Chem. Scand. Ser. B* **1975**, *29*, 353–351. Stewart, W. E.; Siddall, T. H., III *Chem. Rev.* **1970**, *70*, 517–551.

(27) Kalman, J. R.; Blake, T. J.; Williams, D. H.; Feeney, J.; Roberts, G. C. K. *J. Chem. Soc., Perkin Trans. 1* **1979**, 1313–1321. Blake, T. J.; Kalman, J. R.; Williams, D. H.; *Tetrahedron Lett.* **1977**, 2621–2624. Kessler, H.; Rundel, W. *Chem. Ber.* **1968**, *101*, 3350–3357. Ottnad, M.; Hartter, P.; Jung, G. *Z. Physiol. Chem.* **1975**, *356*, 1011–1025.

(28) Conley, R. T. "Infrared Spectroscopy"; Allyn and Bacon: Boston, 1966.

Table IV. HNCH NMR Coupling Constants ($J_{N\alpha}$ Hz) for Roseotoxin B Conformations in the Crystal and in Solution[a,b]

	$J_{N\alpha}$ (θ_{HNCH}), deg	
exptl	9.2 (−169)	8.1 (155)
2a	8.4 (−158)	9.5 (179)
2b	8.0 (−153)[c]	9.3 (173)[c]
3a	9.5 (179)[c]	9.1 (−167)[c]
2a-3a av	8.6	9.3

[a] $CDCl_3$ solvent; ^1H 250 MHz. [b] NMR coupling constants and dihedral angles were related by the modified Karplus equation cited in ref 29 and 30. Thus, the experimental θ_{HNCH} was calculated from the measured J's, while the J's for 2a–3a were calculated from the corresponding angles. [c] θ_{HNCH} angles obtained following the addition of hydrogens with standard bond lengths and angles to the X-ray structures.

buried protons to the molecular surface are decidedly more rapid than conformational interchange. Thus, with or without conformational equilibration, the calculated *relative* exposure should provide a reasonable mixture of solvent access.

For the roseotoxin B conformer with the *sec*-butyl side chain directed toward the periphery of the peptide ring (**2**, Figure 2), the β-Ala NH is calculated to be considerably more accessible to solvent than the Ile NH (Table III). However, for the conformer holding the Ile ethyl fragment over the ring (**3a**, Figure 2), the two internal NH's are found to be nearly equally shielded from solvent. Obviously, the *n* H bond NH experiences an "umbrella effect" as a result of the side-chain rotation from **2** to **3**. What is evident, then, is that roseotoxin B exhibits a blend of several phenomena. In both side-chain conformations, the *m* hydrogen bond (β-Ala NH) is stronger (Table II). However, the same bond is significantly more accessible to solvent in accord with the NMR studies described above. By comparison, the Val NH in structure **4c** is calculated to lie at the molecular surface, in agreement with its large temperature coefficient and relatively rapid exchange in **4b**.

The analysis rests, of course, on the reasonable assumption that the crystal and solution conformations are essentially the same. The two HNCH coupling constants ($J_{N\alpha}$) are supportive. Experimental values[9] are given in Table IV along with those calculated from a Karplus equation designed for assessing peptide structure.[29,30] A simple average of $J_{N\alpha}$'s derived from the X-ray conformations **2a–3a** provides a satisfactory fit. The 1.2-Hz discrepancy at β-alanine does, however, suggest the possibility that a proportion of other conformations may exist in solution.

The apparent disagreement between an assessment of the strengths of the hydrogen bonds *m* and *n* in solution and in the crystal is thereby resolved by invoking an averaged shielding of the NH's from solvent. The geometrically stronger internal bond *m* is simply more exposed to solvent. This, in turn, arises because of the willingness of the roseotoxin B molecule **1**/**1′** to tolerate low-energy backbone distortions induced by side chain conformational averaging.

Isoelectronic and Congeneric Analogues of Roseotoxin B. If the cross-ring hydrogen bonds *m* and *n* are not important for determining the 19-membered ring conformation of **1** as implied by arguments above, their elimination should cause little distortion in the backbone geometry. Accordingly, structures **5–8** were constructed and submitted to MM2 for geometry relaxation. The results, compared with the MM2 optimized version of roseotoxin B (**2c**), are listed in Table V.

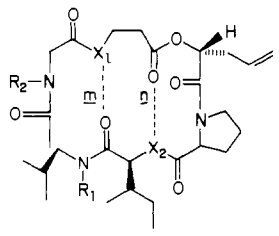

	X_1	X_2	R_1	R_2
1/2c	NH	NH	CH_3	CH_3
4c	NH	NH	H	H
5	O	NH	CH_3	CH_3
6	O	O	"	"
7	polyene		"	"
8	NCH_3	NCH_3	H	H

It is clear that replacement of neither β-Ala NH in *m* nor both NH's of *m* and *n* with oxygen to give the corresponding depsipeptides **5** and **6**, respectively, is sufficient to depopulate the local roseotoxin B ring backbone conformational energy minimum. Although four ϕ/ψ angles in **6** deviate from **2c** by more than 10° (average deviation, ±13°), the overall average deviations for **5** and **6** are 3° and 6°, respectively (Table V). It is noteworthy that the four larger angles all cluster about the atoms representing N—H···O=C in *n* of **1** (ϕ/Ile, Pent; ψ/Pro; ψ/Pro; θ_3/β-Ala). Thus, deletion of both H bonds in **1** is predicted to cause small local backbone adjustments around one of these centers. In the same spirit, transformation of **2c** by replacing each CO—NH amide unit with CH=CH to give hydrocarbon **7** yields precisely the same qualitative result though some of the torsional angles are more seriously affected. In particular, the Ala ϕ/ψ angles are perturbed by 20–30° accompanied by an overall angle deviation from **2c** of ±16°. The differences can be rationalized by considering the stiffened amide and lactone partial double bonds and by the corresponding obligatory bond length and bond angle changes.[31] Importantly, the hydrocarbon shape is basically the same as that for roseotoxin B (Figure 5). In none of these cases has a search for other minima or the global minimum been carried out. The point to be stressed is that hydrogen-bond removal is not accompanied by topologically significant deformation in a given local minimum.

Protodestruxin **4d** exhibits a poorly resolved NMR spectrum evaluated as reflecting an equilibrium between two or more conformations.[23] The lack of similar conformational freedom in **1**/**1′** has been ascribed to a restrictive steric effect associated with the *N*-methyls in the latter but missing in **4d**.[9,23] This property is not evident from the force-field calculations. The optimized desmethyl structure **4c** retains hydrogen bond geometries (Table II) and ϕ/ψ angles (Table V) that are comparable with those of **2c**. The average deviation of the latter is a diminutive ±6°. One small adjustment that perhaps reflects steric compression is a computed 13° reduction in the valine R–N(CH_3)–C_α–C_β dihedral angle from −52° (**2c**, R_1 = CH_3) to −39° (**4c**, R_1 = H). The corresponding angles about Ala *N*-R_2 remain unchanged.

An alternative suggestion for the conformational mobility of the demethylated dipsipeptide **4d** is more likely: if NH's are found at valine and alanine as well as at isoleucine and β-alanine, other conformations with these residues participating in cross-ring hydrogen bonds become energetically feasible.[23] In the context of the present calculations, however, it would appear that the postulated new conformers are less stabilized by hydrogen bonds than **1**/**1′** is destabilized by the steric congestion afforded by internal *N*-methyl groups. To test this view rigorously, conformations of roseotoxin B with one or both of the Val and Ala *N*-methyls internal to the ring would be needed for computational evaluation. However, a crude measure of the effect can be obtained as follows. The low-temperature X-ray roseotoxin B structure (REH-LT, **1**/**2a**) was supplemented with internal *N*-methyls at Ile and β-Ala, relieved of external methyls at the NH's of Val and Ala, and geometry optimized with MM2 to give conformation **8**. The latter comes about by the N–CH_3's at

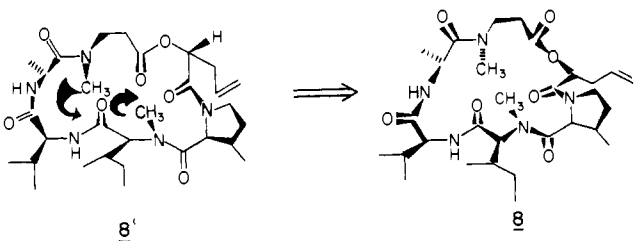

8′ 8

(29) Ramachandran, G. N.; Chandrasekaran, R.; Kopple, K. D. *Biopolymers* **1971**, *10*, 2113–2131.

(30) The modified Karplus equation of ref 29 has been programmed and installed on the Merck Molecular Modeling System by Dr. E. F. McIntyre.

(31) Freidinger, R. M.; Veber, D. F. *J. Am. Chem. Soc.* **1979**, *101*, 6129–6131. Hann, M. M.; Sammes, P. G.; Kennewell, P. D.; Taylor, J. B.; *J. Chem. Soc., Perkin Trans. 1* **1982**, 307–314.

Table V. Dihedral Angles (deg) for MM2-Optimized Structures Isoelectronic and Congeneric with Roseotoxin B[a]

		2c	4c	5	6	7	8
Ile,	ϕ	−76	−79	−72	−58	−95	−93
	ψ	135	138	140	138	143	135
	ω	168	173	166	164	176	178
Val,	ϕ	−92	−91	−98	−97	−93	−51
	ψ	95	101	94	95	102	108
	ω	22	2	21	20	2	−2
Ala,	ϕ	−138	−125	−140	−141	−121	−129
	ψ	84	103	87	88	115	159
	ω	178	−178	173	173	180	175
β-Ala,	$\theta 1$	−115	−132	−114	−115	−128	160
	$\theta 2$	−72	−66	−73	−72	−77	−57
	$\theta 3$	171	156	167	160	121	119
	LACTONE	174	172	175	176	177	176
Pent,	ϕ	53	55	58	64	89	62
	ψ	−127	−126	−127	−131	−127	−135
	ω	−175	−173	−174	−174	−179	−155
Pro,	ϕ	−81	−79	−81	−75	−82	−53
	ψ	−17	−16	−19	−30	7	−54
	ω	179	176	176	170	179	−174
$\phi/\psi/\omega$ deviation from 2c[b]			7	3	7	16	30

[a] The Ile and hydroxy-Pent side chains are in the same conformation as for 2c (Table I). [b] Absolute values of the average deviations of the $\phi/\psi/\theta$ angles from those for 2c.

β-alanine and isoleucine twisting down under and up over the average plane of the molecule, respectively. The corresponding cross-ring C=O's of the same residues react accordingly.

As shown by the dihedral angles of Table V, significant changes relative to **2c** are sustained in the ring backbone at all residues. In addition, structure **8** is 6 kcal less stable than the latter, in agreement with the destabilization argument given above. A small part of the energy gap is undoubtedly attributable to the constitutional differences between **1**/**2c** and **8**. The reader should note that by no means can the latter be considered a global conformational minimum as its potential energy surface has been sampled only in this single molecular shape.

Conclusions

Cross-ring intramolecular hydrogen bonding in **1**/**1′** does not appear to exert a strong influence on the conformational shape of roseotoxin B. The 19-membered ring breathes easily as the attachments implied by *m* and *n* undergo stretching and compression in response to even small torsional displacements about the Cα–Cβ Ile bond. Both experiment and molecular mechanics theory coincide on this point. The shorter bond, *m*, is the more NMR active, another echo of the low-energy side-chain mobility. Eradication of *m* and *n* altogether by modeling double and triple lactones **5** and **6** and polyene **7** provides additional support for conformational stability separate from H bonding. The significance of these numerical experiments is the insight that intramolecular hydrogen bonding most likely affects only *local* conformational properties that are not transmitted to the cyclic polyamide ribbon as a whole.

The suggestion that hydrogen bonding is without strong consequence in roseotoxin B and by implication in other cyclic peptides of similar size is made with some reservation. Karlson has written that "hydrogen bonds can be taken to be the most important secondary valence forces that maintain the conformation of the protein molecule".[32] Though N–H···O interactions are weak, amounting to about one-twentieth the energy of a covalent bond, their large number makes a decisive contribution to the determination of molecular geometry. Perhaps equally important, hydrogen bonding in proteins is cooperative and may enhance bond energies by as much as 25%.[33] Further, essential properties of biological polymers depending on cross-linking and specific folding influences are intimately guided by hydrogen bonds.[34] And finally, the dynamics of many biological transformations are undoubtedly dependent on the weak nature of hydrogen bonds. Processes such as enzyme binding and DNA replication, for example, require temporary molecular superposition coupled to rapid particle release and efficient recycling.

For small cyclic peptides the balance of forces prejudices the hydrogen bonds to play a considerably reduced role. On the one hand, there are far fewer of them, only two in the present case. Secondly, ring formation introduces a serious constraint that obligates geometric coupling among all the residues in the molecule. This is of particular moment for a substance like roseotoxin B where the ring contains six relatively stiff partial double bonds, a proline rigidifier, and a collection of sterically demanding side chains. While there is not yet a great deal of information concerning energy barriers separating cyclic peptide conformations,[1b,25-27] the transition-state energies, nonetheless, most certainly contain prominent contributions from the latter structural factors. Conversely, the depth of the conformational energy wells and the molecular shapes found there are equally dependent on them. This implies that in a rigid molecular frame inside a pocket unexposed to solvent, hydrogen bonds can be expected to form effectively by default. The cycle thereby confers stability on the hydrogen bond, rather than the reverse.

Indirect support for this thesis is to be found among X-ray determinations for cyclic hexapeptides and isostructural systems. One of the most persistent backbone conformations for the former in the solid state contains two β-turns and two extended connecting residues.[5a,35] A principal stabilizing factor has come to be recognized as a β-turn incorporating a strong 4→1 hydrogen bond.[5-7] An early exception was found in the structure of cyclic hexaglycyl. Four separate conformations are found in the unit cell, only one of which possesses the geometric features associated with cross-ring hydrogen bonding.[20a] Similarly, *cyclo*-(L-Leu-L-Tyr-δ-Aveler-δ-Aveler), a synthetic inhibitor of chymotrypsin and a ring-mimic of a cyclic hexapeptide, adopts a conformation very similar to one of those found for cyclic hexaglycyl.[36] However, it is one of the three that does not evidence intramolecular H bonding.

Recently, the presence of the β-turn geometry, but the absence of the expected hydrogen bond have elicited comment from several groups of workers. For example, both *cyclo*(Ala-Pro-D-Phe)$_2$ with C_2 symmetry and *cyclo*(Gly-Pro-D-Phe)$_2$ sustain a pair of type

(32) Karlson, P. "Introduction to Modern Biochemistry"; Academic Press: New York, 1968; p 46.
(33) Hinton, J. F.; Harpool, R. D. *J. Am. Chem. Soc.* **1977**, *99*, 349–353. Sheridan, R. P.; Lee, R. H.; Peters, N.; Allen, L. C.; *Biopolymers* **1979**, *18*, 2451–2458. Mehler, E. L.; *J. Am. Chem. Soc.* **1980**, *102*, 4051–4056.
(34) Schulz, G. E.; Schirmer, R. H. "Principles of Protein Structure"; Springer-Verlag: New York, 1979; p 174.
(35) Yang, C. H.; Brown, J. N.; Kopple, K. D. *J. Am. Chem. Soc.* **1981**, *103*, 1715–1719.
(36) Karle, I. L. *Macromolecules* **1976**, *9*, 61–66.

II β-turns, but neither shows cross-ring bonding.[37] The proline-containing substances *cyclo*(Gly-Pro-XXX)$_2$ (XXX = D-Ala, Gly) exhibit two β-turns but are unsymmetrical and reveal only one intramolecular hydrogen bond in the crystalline state.[38] In all of these cases geometric analysis suggested that unfavorable O···O repulsions induced by the ring conformation prevent close approach of the β-turn N—H/O=C moieties. This effect was predicted earlier by Madison as a consequence of electrostatic repulsion between contiguous cross-ring hydrogen bonds in the cyclic array.[39] Complementary NMR studies, however, have indicated C_2 symmetry in solution where asymmetry exists in the solid.[40] The proline-free hexapeptide *cycl*(Gly-D-Leu-Leu)$_2$ evidences similar properties. Two crystallographically independent molecules are found in the unit cell,[20b] Each possesses two β-turns but only one 4→1 intramolecular hydrogen bond. NMR and CD spectroscopy indicate that one of these most likely equilibrates with yet another conformer in solution. In general, conformational homogeneity in the solid accompanied by conformer averaging in solution is not uncommon.[35] In corroboration, a careful NMR investigation of a series of cyclic hexapeptides led Gierasch to the conclusion that 1,4-hydrogen bonding in the β-turn "is not a strong effect".[41]

These and other studies[42] clearly reveal that β-turns may or may not support hydrogen bonding. When the 4→1 links are manifest, their structural framework can exist side by side both in the crystal and in solution with other conformations that do not require intramolecular hydrogen bonds. The energy difference between the cross-linked and the cross-link-free structures is therefore diminishingly small. Under the circumstances, it is difficult to argue that hydrogen bonding is a serious structural determinant for cyclic hexapeptides. The results for roseotoxin B described above suggest it to be a prototype for the overwhelming importance of ring conformation factors. These, in turn, must be evaluated in terms of torsional freedom, internal dipole interactions, and medium effects.[44] It remains to be seen how structural composition and ring size in cyclic peptides in general partition the various energy components insofar as they contribute to conformational integrity.

Acknowledgment. I thank Prof. Garland Marshall (Washington University School of Medicine, St. Louis) for early access to the MM2 amide parameters and Dr. Jim Springer for providing the roseotoxin B X-ray results prior to publication. Drs. Peter Gund, Tom Halgren, and Bruce Bush (Merck) engaged in stimulating and valuable discussions.

Registry No. 1, 55466-29-0; **4a**, 2503-26-6; **4b**, 27482-48-0; **4c**, 88945-79-3; **4d**, 88945-80-6; **5**, 88945-81-7; **6**, 88945-82-8; **7**, 88945-84-0; **8**, 88945-83-9.

(37) Brown, J. N.; Teller, R. G. *J. Am. Chem. Soc.* **1976**, *98*, 7565-7569. Brown, J. N.; Yang, C. H. *Ibid.* **1979**, *101*, 445-449.
(38) Kostansek, E. C.; Lipscomb, W. N.; Thiessen, W. E.; *J. Am. Chem. Soc.* **1979**, *101*, 834-837. Kostansek, E. C.; Thiessen, W. E.; Schomburg, D.; Lipscomb, W. N. *Ibid.* **1979**, *101*, 5811-5815.
(39) Madison, V. S. "Peptides, Polypeptides and Proteins"; Blout, E. R.; Bovey, M.; Goodman, M.; Lotan, N., Eds.; Wiley-Interscience: New York, 1974; pp 89-98.
(40) (a) Pease, L. (presently Gierasch, L.) Ph.D. Thesis, Harvard University, 1975. (b) Pease, L.; Deber, C. M.; Blout, E. *J. Am. Chem. Soc.* **1973**, *95*, 258-260. Schwyzer, R.; Grathwohl, C.; Meraldi, J. P.; Tun-Kyi, A.; Vogel, R. Wüthrich, K. *Helv. Chim. Acta.* **1972**, *55*, 2545-2549.
(41) Pease, L. ref 40a, p 254.
(42) Evidence has been reported that the same may be said for γ-turns in cyclic pentapeptides as well.[43]
(43) Karle, I. L. *J. Am. Chem. Soc.* **1979**, *101*, 181-184. Pease, L. G.; Niu, C. H.; Zimmerman, G. *Ibid.* **1979**, *101*, 184-191.
(44) Kopple, K. D.; Schamper, T. J.; Go, A. *J. Am. Chem. Soc.* **1974**, *96*, 2597-2605.

Systematic Approach to the Analysis of Carbon-13 NMR Spectra of Complex Carbohydrates. 1. α-D-Mannopyranosyl Residues in Oligosaccharides and Their Implications for Studies of Glycoproteins and Glycopeptides

Adam Allerhand* and Elisha Berman

Contribution from the Department of Chemistry, Indiana University, Bloomington, Indiana 47405. *Received October 12, 1982*

Abstract: The ^{13}C NMR spectra (at 67.9 MHz) and specific assignments of the ^{13}C resonances are presented for Manα1→2Man, Manα1→2Manα1→2Man, Manα1→2Manα1→2Manα1→2Man, Manα1→3Manα1→2Manα1→2Man, Manα1→4Manα1→0CH$_3$, Manα1→6Manα1→6Man, and the linear (1→6)-α-D-mannopyranan. It is shown that the chemical shifts of all the carbons of a nonreducing α-D-mannopyranose residue are substantially influenced by the nature of the group to which the terminal residue is linked. For example, when going from a Manα1→4Man(α) moiety to Manα1→6Man(α), there are substantial changes in the chemical shifts of all carbons (excpet C-6) of the nonreducing terminal mannose. The α-D-mannosylation of an α- or β-D-mannopyranosyl residue at C-2, C-3, C-4, or C-6 also causes significant changes in the chemical shifts of most carbons of the mannosylated residue. A method is presented for calculating the chemical shifts of any α-D-mannopyranosyl residue linked to other α-D-mannopyranosyl residues (at C-1, C-2, C-3, C-4, or C-6 or any combination of such linkages), on the basis of the chemical shifts of the oligosaccharides listed above. For this purpose, two sets of data are presented: (i) the chemical shifts of nonreducing terminal α-D-mannopyranosyl residues involved in 1→2, 1→3, 1→4, and 1→6 linkages to other α-D-mannopyranosyl residues and (ii) the effects of α-D-mannosylation at C-2, C-3, C-4, and C-6 of an α-D-mannopyranosyl residue. The predictive powers of these two empirical data sets are tested by comparing the experimental and calculated spectra of the α-D-mannopyranosyl residues of Manα1→6(Manα1→3)Manα1→6Manβ1→R, where R = 4GlcNAcβ1→4GlcNAcβ1→Asn. There is very good agreement between the experimental and calculated spectra, to the point that the calculated spectra are readily used to rule out alternate structures such as Manα1→6Manα1→6(Manα1→3)Manβ1→R, on the basis of differences in several regions of the spectrum. It is shown that high-field superconducting NMR spectrometers provide enough resolution in the ^{13}C NMR spectra of complex carbohydrates to allow extensive use of the nonanomeric carbon resonances (and not just those of the anomeric carbons) in structural studies of large oligosaccharides.

The determination of the primary structure of the carbohydrate side chains of glycoproteins is usually a formidable task, both because the available methods are time consuming and often ambiguous and because glycoprotein heterogeneity often greatly

0002-7863/84/1506-2400$01.50/0